Journal of Cell Science 108, 3039-3050 (1995)
Printed in Great Britain © The Company of Biologists Limited 1995

Intracellular transport of the murine leukemia virus during acute infection of NIH 3T3 cells: nuclear import of nucleocapsid protein and integrase

Cristina Risco[1,2,*], Luis Menéndez-Arias[3,†], Terry D. Copeland[4], Pedro Pinto da Silva[2] and Stephen Oroszlan[3]

[1]Biological Carcinogenesis and Development Program, Program Resources, Inc./Dyncorp, [2]Membrane Biology Section, Laboratory of Mathematical Biology, National Cancer Institute, [3]Laboratory of Molecular Virology and Carcinogenesis, and [4]Protein Chemistry Group, ABL-Basic Research Program, Frederick Cancer Research and Development Center, Frederick, MD 21702-1201, USA

*Author for correspondence at present address: Centro Nacional de Biotecnología, CSIC, Campus Universidad Autónoma de Madrid, Cantoblanco, 28049 Madrid, Spain
†Present address: Centro de Biología Molecular 'Severo Ochoa', Consejo Superior de Investigaciones Científicas-Universidad Autónoma de Madrid, 28049 Cantoblanco (Madrid), Spain

SUMMARY

The entry and intracellular transport of Moloney-murine leukemia virions inside mouse NIH 3T3 cells have been followed by electron microscopy techniques. Five viral proteins - matrix (MA, p15), capsid (CA, p30), nucleocapsid (NC, p10), integrase (IN), and the envelope glycoprotein (SU, gp70) - were located by immunolabeling using gold probes. After entering the cells, viral particles were frequently detected inside cytoplasmic vesicles of variable size. Their viral envelope was apparently lost during intracytoplasmic transport. When the unenveloped viral cores reached the nuclear membrane or its vicinity, they were disrupted. Two of the immunolabeled proteins, NC and IN, were detected entering the nucleus of non-dividing cells, where both were targeted to the nucleolus. However, MA and CA were found only in the cytoplasm. NC is a nucleic acid-binding protein which contains potential nuclear localization signals. We suggest that NC could enter the nucleus as part of a nucleoprotein complex, associated with IN, and possibly, also with viral DNA.

Key words: MuLV, NC protein, immunogold

INTRODUCTION

The early phase of the retroviral life cycle involves a series of sequential events starting with the attachment of a virion to a receptor on the cell surface. Then, viruses are internalized either by direct fusion of viral and cell membranes at neutral pH or by an endocytic (pH-dependent) pathway (Andersen and Nexø, 1983; Marsh and Helenius, 1989; Luciw and Leung, 1992; Ragheb and Anderson, 1994). The entry process releases the virion core into the cell cytoplasm, where additional uncoating events take place, and reverse transcription is initiated (Varmus and Swanstrom, 1982). The proviral DNA, which can exist in a linear or circularized form, must integrate into the host chromosomal DNA to complete the infection of the cell (Luciw and Leung, 1992). Nucleoprotein complexes with integration activity in vitro, have been isolated from the cytoplasm of cells acutely infected with murine leukemia virus (MuLV) (Bowerman et al., 1989). These integration-competent complexes have a large molecular mass (sedimentation coefficient: 160 S) and contain viral DNA, as well as integrase (IN) and capsid protein (CA). Little is known on the extent of the uncoating process and the fate of the MuLV core proteins, upon entering the cell.

Immunogold labeling techniques combined with electron microscopy have shown high resolution and sensitivity for the visualization of molecules in viruses and the intracellular environment (Carracosa et al., 1986; Gelderblom et al., 1987; Carrascosa, 1988; Menéndez-Arias et al., 1992; Risco and Pinto da Silva, 1995). In this work, we used immunoelectron microscopy to follow the early events of Moloney-MuLV infection of NIH 3T3 cells. Specific polyclonal antibodies which recognize the viral proteins MA, CA, NC, IN, and gp70, were used to follow the fate of these proteins inside the cells. Our study shows that after disruption of the viral core at the cytoplasmic face of the nuclear membrane, NC and IN can enter the nucleus of non-dividing cells, where they accumulate preferentially at the nucleoli.

MATERIALS AND METHODS

Cells and infections

Uninfected NIH 3T3 cells (American Type Culture Collection CRL 1658) were cultured in Dulbecco's modified Eagle's medium supplemented with 10% donor calf serum (C-DMEM) and maintained at 37°C in a humidified atmosphere containing 5% CO_2. TR295E

cultures, obtained after transfection of CHO cells with a protease-deficient Moloney-MuLV clone (Fu and Rein, 1993) were provided by Alan Rein, and grown in 90% α-modified minimum essential medium, 10% fetal calf serum, in the presence of 0.2 mg/l of G418. Moloney-MuLV was harvested from NIH 3T3 cells productively infected with wild-type virus. After centrifugation of culture supernatants at 140,000 ***g*** for 60 minutes at 4°C using a Beckman type 45 Ti rotor, the virus was resuspended in C-DMEM. Infections were done in 10 cm diameter plates containing around 5×10^6 uninfected (80% confluency) NIH 3T3 cells. An electron microscopy analysis of these cultures revealed that less than 0.1% of these cells were in mitosis. Before adding the virus, cultures were maintained at 37°C for 30 minutes in the presence of Polybrene (25 μg/ml). After washing the monolayers with C-DMEM, the cultures were cooled to 4°C for 15 minutes, and were inoculated with a concentrated virus suspension (approx. 10^{10} viral particles/plate). Viral adsorption was carried out at 4°C for 60 minutes with occasional swirling. Then, cultures were washed, warmed quickly to 37°C by addition of prewarmed C-DMEM, and incubated at that temperature for 0, 0.5, 1, 1.5 and 3 hours.

The number of viral particles/ml was estimated by electron microscopy after negative staining with 1% uranyl acetate. This was done after mixing an aliquot of the viral concentrate at an appropriate dilution with an equal volume of a suspension of latex spheres of known concentration (2.41×10^{10} particles/ml) and homogeneous size (0.0910±0.0058 μm), obtained from Ernest F. Fullam, Inc. (Latham, NY).

RT activity of culture supernatants of newly infected cells was monitored during the following 14 days after infection, using $(dT)_{15}\cdot(A)_n$ as the primer template and Mn^{2+} as the divalent cation (Poiesz et al., 1980). As expected, significant amounts of RT activity were already detected 3-5 days after exposure to MuLV.

All the cell lines used in this study were known to be free of mycoplasma contamination.

Antisera

Immunogold localization of the MuLV proteins MA and CA was carried out using polyclonal antisera raised against the purified viral proteins. Goat polyclonal antisera specific for MA and gp70, and guinea pig antiserum specific for CA were available in our laboratory from previous studies. Rabbit and guinea pig polyclonal antisera recognizing the NC protein were raised against the synthetic peptides SP-614 ($ATVVSGQKQDRQGGEC_{amide}$) and SP-1429 (CPRGPRG-PRPQTSLL), which correspond to the amino- and carboxyl-terminal regions of NC. These peptides were coupled to keyhole limpet hemocyanin (KLH; Calbiochem) through their cysteine residues by reaction with *m*-maleimidobenzoyl-*N*-hydroxysuccinimide ester (MBS) (Pierce). Rabbit polyclonal antiserum recognizing the viral IN was obtained after immunization with a synthetic peptide whose sequence corresponds to the IN residues 20-38 (KDLTKLGAIYDKTKKY-$WVYC_{amide}$), which was previously coupled to KLH. No cross-reactivity with other viral proteins was observed in western blot assays.

Thin-section electron microscopy for ultrastructural studies

Virus-treated NIH 3T3 cultures were fixed in situ with 1% glutaraldehyde in phosphate buffered saline (PBS) for 1 hour at room temperature, and then postfixed and processed for Epon-embedding as previously described (Risco et al., 1994).

Immunoelectron microscopy

Low temperature embedding in Lowicryl K4M

For immunolabeling of viral proteins, infected and uninfected cultures of NIH 3T3 cells were washed with C-DMEM and fixed in situ at 4°C with a solution of 4% paraformaldehyde, 0.1% glutaraldehyde in PBS, for 15 minutes at 4°C. After extensive washing with PBS, the cells were incubated for 20 minutes with a solution of 0.2 M ammonium chloride, to block any possible free aldehyde groups that may remain in the preparations. After two washes of 10 minutes each with PBS, cells were dehydrated by treatment with 30% ethanol (20 minutes, 4°C) and then with 50, 70, 90% ethanol, and twice with 100% ethanol (30 minutes, −20°C). Samples were then treated at −20°C with a mixture of Lowicryl K4M:ethanol (1:1) for 1 hour, Lowicryl K4M:ethanol (2:1) for 1 hour, followed by an overnight incubation in 100% Lowicryl. After replacing the resin with a fresh one, samples were kept at −20°C for 8 hours. Finally, the samples were transferred to capsules and polymerized with ultraviolet light in a Ted Pella UV criochamber, for two days at −20°C, and one day at room temperature. Thin-sections of the samples were collected in gold grids covered with Formvar and carbon, and processed for immunolabeling.

Single labeling experiments

Lowicryl thin-sections of NIH 3T3 cells were processed for immunogold labeling as previously described (Menéndez-Arias et al., 1992; Risco et al., 1991; Risco and Pinto da Silva, 1993). The different steps of the immunolabeling procedure were carefully adjusted for each of the antisera in order to obtain maximum labeling with the absence of unspecific background. Together with conventional immunocytochemical controls, such as the use of non-immune sera and incubations in the absence of primary antibodies, sections of noninfected control cells were submitted to the same treatments as sections of MuLV infected cells in all labeling experiments. Only the immunolabeling protocols that rendered a total absence of nonspecific background in these control cells were considered. In all cases immunolabeling was done at room temperature with gentle shaking, starting with a saturation step to block unspecific binding of the reagents to the sections. It included a 30 minute incubation with saturation buffer (PBS containing 0.5 M NaCl, 0.1% bovine serum albumin (BSA), and 0.1% Tween-20), followed by another 30 minute incubation with 5% non-immune serum. Samples were then floated for 90 minutes on a drop of the specific primary antiserum, diluted in saturation buffer (1:100 for rabbit anti-NC antisera, 1:40 for guinea pig anti-NC antisera, 1:300 for guinea pig anti-CA antiserum, 1:1000 for goat anti-MA antiserum, 1:8 for rabbit anti-IN antiserum, and 1:30 for goat anti-gp70 antiserum). After jet-washing with PBS containing 0.5 M NaCl, grids were floated on four drops of the same buffer and vigorously shaken for 5 minutes on each drop. A short saturation step was then applied (10 minutes with saturation buffer, and 10 minutes more with 5% non-immune serum) before a 45 minute incubation with a secondary antibody (goat anti-rabbit IgG, rabbit anti-goat IgG, or goat anti-guinea pig IgG), conjugated with colloidal gold of 10 nm. For labeling IN, a goat anti-rabbit IgG conjugated with 5 nm colloidal gold particles was also used. Washing was repeated as before and grids were then floated on several drops of distilled water before staining with a solution of saturated uranyl acetate for 8 minutes. After washing with distilled water and air drying, samples were studied by electron microscopy.

Double labeling experiments

For simultaneous localization of two proteins or two regions of the same protein, we used primary antibodies raised in two different hosts and secondary antibodies conjugated with gold particles of two different sizes (5 or 10 nm). Saturation, incubation times with the different reagents and washing steps were done as described for single labeling experiments, but the number of steps of the procedure were adjusted to avoid masking of one antigen by antibodies bound to the other. When labeling simultaneously both amino- and carboxyl-terminal regions of NC, samples were incubated with a mixture of the primary antisera (rabbit anti-SP-614, and guinea pig anti-SP-1429, diluted at 1:100 and 1:40, respectively, in saturation buffer). The corresponding secondary antibodies conjugated with colloidal gold were also mixed (diluted 1:40 in saturation buffer). When colabeling NC and CA, double labeling was done in three steps, because when both

primary antibodies were mixed, the amount of labeling associated with NC was significantly reduced. Thus, samples were sequentially incubated with a rabbit antiserum against the amino- or carboxyl-terminal region of NC (diluted 1:80 in saturation buffer), a guinea pig anti-CA (1:250 in saturation buffer), and a mixture of the corresponding secondary antibodies conjugated with 5 or 10 nm colloidal gold (diluted at 1:40 each in saturation buffer). Finally when simultaneously labeling IN and NC, the procedure was done in four steps, as integrase had to be labeled first with the corresponding antiserum and gold conjugate, to avoid masking of this protein by the antibodies against NC.

RESULTS

MuLV entry and intracellular distribution of viral proteins in newly infected mouse NIH 3T3 cells

Immunogold and ultrastructural electron microscopy studies were used to follow MuLV particles in NIH 3T3 cells shortly after addition of the virus to the cells. Five of the viral proteins - NC (p10), CA (p30), MA (p15), IN, and gp70 - were specifically immunodetected in the virions, using polyclonal antibodies raised in different hosts (Fig. 1B-G). All of these antisera (except the one directed to gp70) also recognized their respective protein domains in the Gag and Gag-Pol polyproteins of immature viruses and budding viral particles observed in chronically infected NIH 3T3 cells, as well as in TR295E cultures expressing protease-deficient MuLV (Fig. 1H-J). Sometimes the gold particles were visualized at a certain distance from the capsid (Fig. 1D). This is related to the size of the immunocomplexes and the degree of their extension during the drying of the section. For example, when using 10 nm gold particles and two immunoglobulin molecules the distance between gold marker and antigen is about 18-28 nm (Kellenberger and Hayat, 1991).

We have confirmed that it is difficult to follow the virions inside the cytoplasm solely by morphological criteria in sections of EM resins for ultrastructure, as previously reported (Miyamoto and Gilden, 1971). However, immunogold labeling of subviral components allowed a precise detection of MuLV in the cytoplasmic environment of the cells visualized in Lowicryl sections.

Individual MuLV or groups of viruses were incorporated by NIH 3T3 cells inside vesicles of variable size (Figs 2 and 3A). Progressive binding and uptake of virions by the cells were observed. Thus, the percentage of cells with more than 5 intracellular viruses (as visualized in thin-sections) increased from 3% in cells incubated with the virus for 30 minutes, to 46% after 3 hours of treatment at 37°C. However, in the same time interval, we observed little change in the percentage of cells having viruses attached to their plasma membrane (from 70% to 86%), suggesting that binding is fast but intracellular accumulation is slower. Once the virus enters the cell, we observed the release of some viral particles from the vesicles into the cytoplasm (Fig. 3B). This process may represent the loss of the viral envelope by fusion with the vesicular membrane, as a decrease in diameter (compared to extracellular viruses) is morphologically obvious in intracytoplasmic virions (their diameter is approximately 45-65 nm, in contrast to 100 nm for extracellular viruses). We have also observed the loss of the immunogold labeling associated with the envelope glycoprotein gp70 (SU) in viral particles reaching the cell nucleus. Thus, 71% of the extracellular and 68% of the intravesicular viruses were labeled with the anti-gp70 antiserum, but only 20% of the viral particles released into the cytoplasm were detected with such an antiserum. In addition, we observed a decrease in labeling intensity. The average number of gold particles per labeled virus was 2.8 for extracellular and intravesicular virions, and 1.1 for intracytoplasmic cores. Cores having two associated gold particles were rare (less than 4%). However, more than 75% of the extracellular and intravesicular viruses observed contained at least two gold particles. The virions appear then to reach the nucleus as unenveloped viral cores that remain basically intact during their transport across the cytoplasm, as indicated by immunogold labeling of NC, CA, MA, and IN. The average number of gold particles associated with these proteins was similar in extracellular virions as compared to viral cores close to the nuclear envelope. Moreover, there was no increase of free gold labeling in the

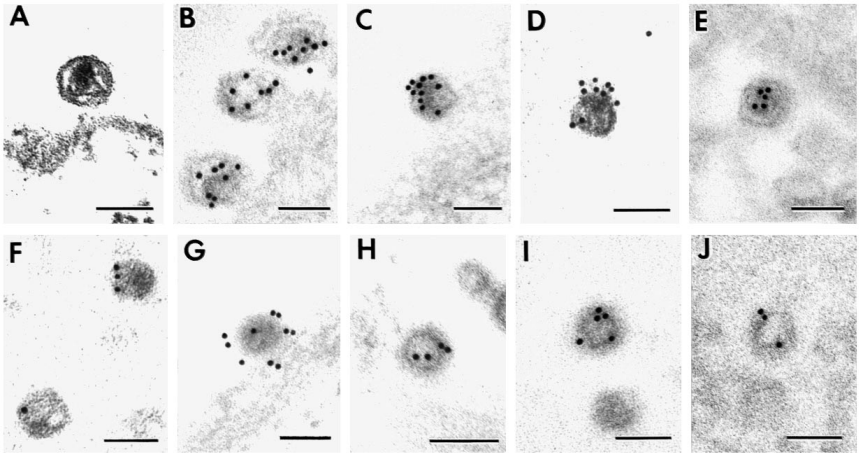

Fig. 1. Ultrastructure of murine leukemia virus and immunogold localization of its proteins. From (A) to (G) viral particles from acutely infected NIH 3T3 cells are shown. (A) shows a viral particle as observed in Epon sections of samples fixed with 1% glutaraldehyde. (B-G) show the detection of viral proteins in mature virions by immunogold labeling on Lowicryl sections of material fixed in mild conditions: (B) CA, detected with a guinea pig polyclonal antiserum. (C) MA labeled with a goat polyclonal antiserum. (D) NC labeled with a rabbit antiserum raised against the amino-terminal region of the protein. (E) Carboxyl-terminal region of the NC protein, labeled with a guinea pig antiserum. (F) IN was labeled with a rabbit polyclonal antiserum, and appears in a smaller amount due to the lower number of molecules incorporated into virions as compared to *gag*-encoded proteins. (G) Localization of gp70 (SU), using a goat polyclonal antiserum. (H) and (I) Detection of NC and CA, respectively, in immature protease-deficient MuLV particles (released by TR295E cultures), with the antisera indicated in (D) and (B), respectively. (J) Localization of MA (with the antiserum indicated in C) in an immature virus from chronically infected NIH 3T3 cultures. Gold conjugates shown in this figure correspond to 10 nm particle size. Bars, 100 nm.

cytoplasm, which could indicate a release of viral proteins from disrupted viruses. These facts indicate that no major disruption of virus structure, or loss of particular proteins occurs. When reaching the nuclear envelope or its vicinity, the viral cores are disrupted and lose their structure. Immunogold labeling showed the presence of viral proteins (e.g. NC) associated with these subviral structures located at the interphase cytoplasm-nucleus (see arrow in Fig. 3C). Two of the immunolabeled MuLV proteins were later detected inside the nucleus: NC and IN.

Release and intranuclear distribution of MuLV NC

The disruption of the viral cores at the nuclear envelope is associated with the presence of intranuclear aggregates of NC (Fig. 3C,D). NC-containing complexes seem to enter the nucleus through the nuclear pores, as labeling associated with NC was detected in the center and periphery of these structures (Fig. 3E,F). MuLV also reaches the nucleus inside vesicles containing large groups of viral particles (Fig. 4A,B), similar to those observed in cells infected by the polyomavirus SV40 (Mackay and Consigli, 1976; Nishimura et al., 1986). In SV40, this vesicular transport leads to a massive release of viruses into the nucleus. In case of MuLV, the intravesicular viral particles appear to be transported to the cytoplasmic side of the nuclear envelope (Fig. 4B), although we could not obtain any ultrastructural evidence of a release of viral aggregates or capsids from the vesicles into the nucleus.

After 30 minutes incubation at 37°C, following the addition

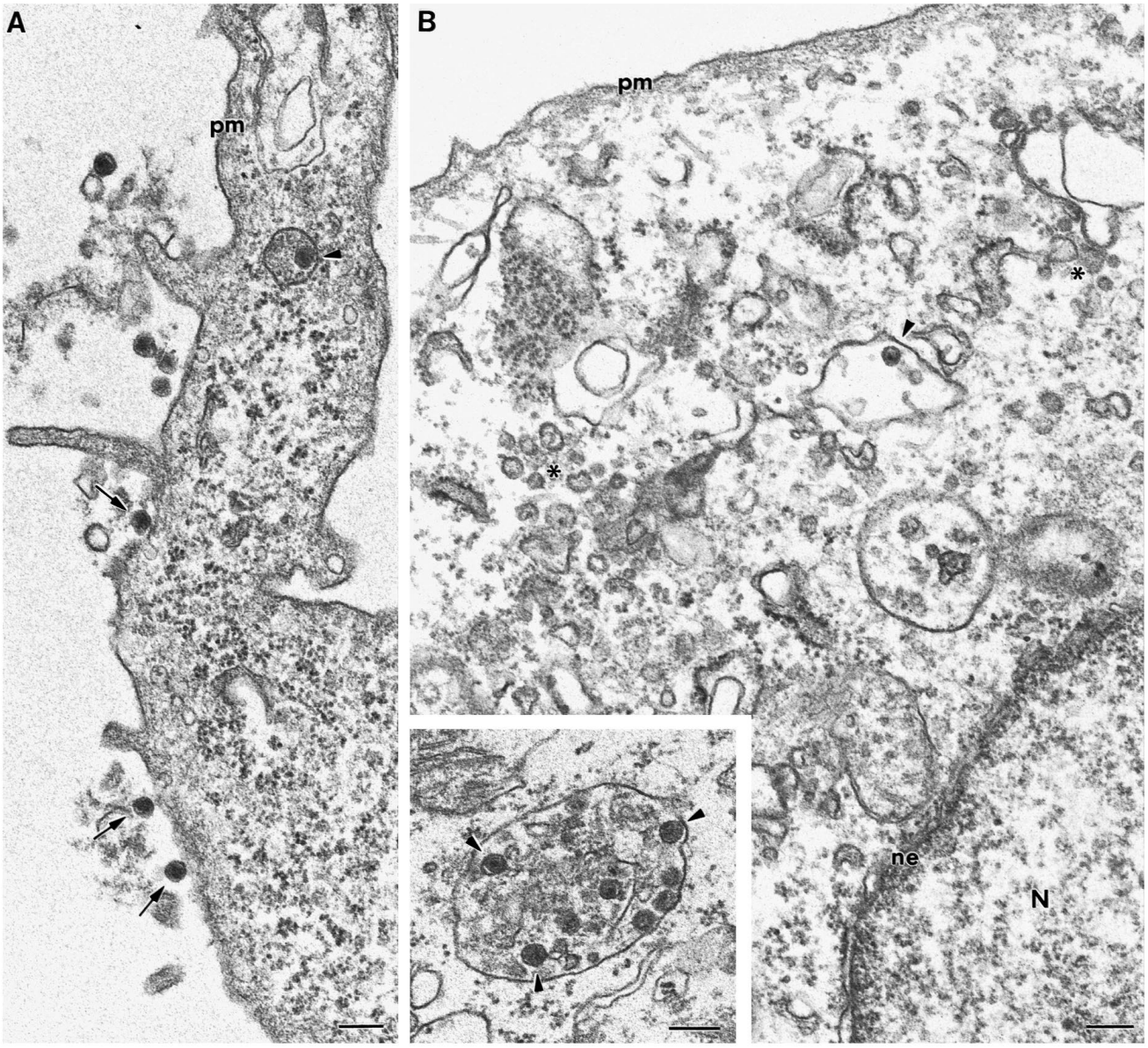

Fig. 2. Ultrastructure of MuLV-treated NIH 3T3 cells. (A) Epon ultrathin sections show viral particles attached to the plasma membrane (arrows) and inside cytoplasmic vesicles (arrowhead). Cells were collected 30 minutes after treatment with MuLV. (B) General view of the cytoplasm of NIH 3T3 cells 50 minutes after treatment with the virus. A complex system of vesicles and granules (asterisks) characterizes these cells. In this environment viral particles are clearly identified only when located inside vesicles (arrowheads in mainfield and inset). pm, plasma membrane; ne, nuclear envelope; N, nucleus. Bars, 200 nm.

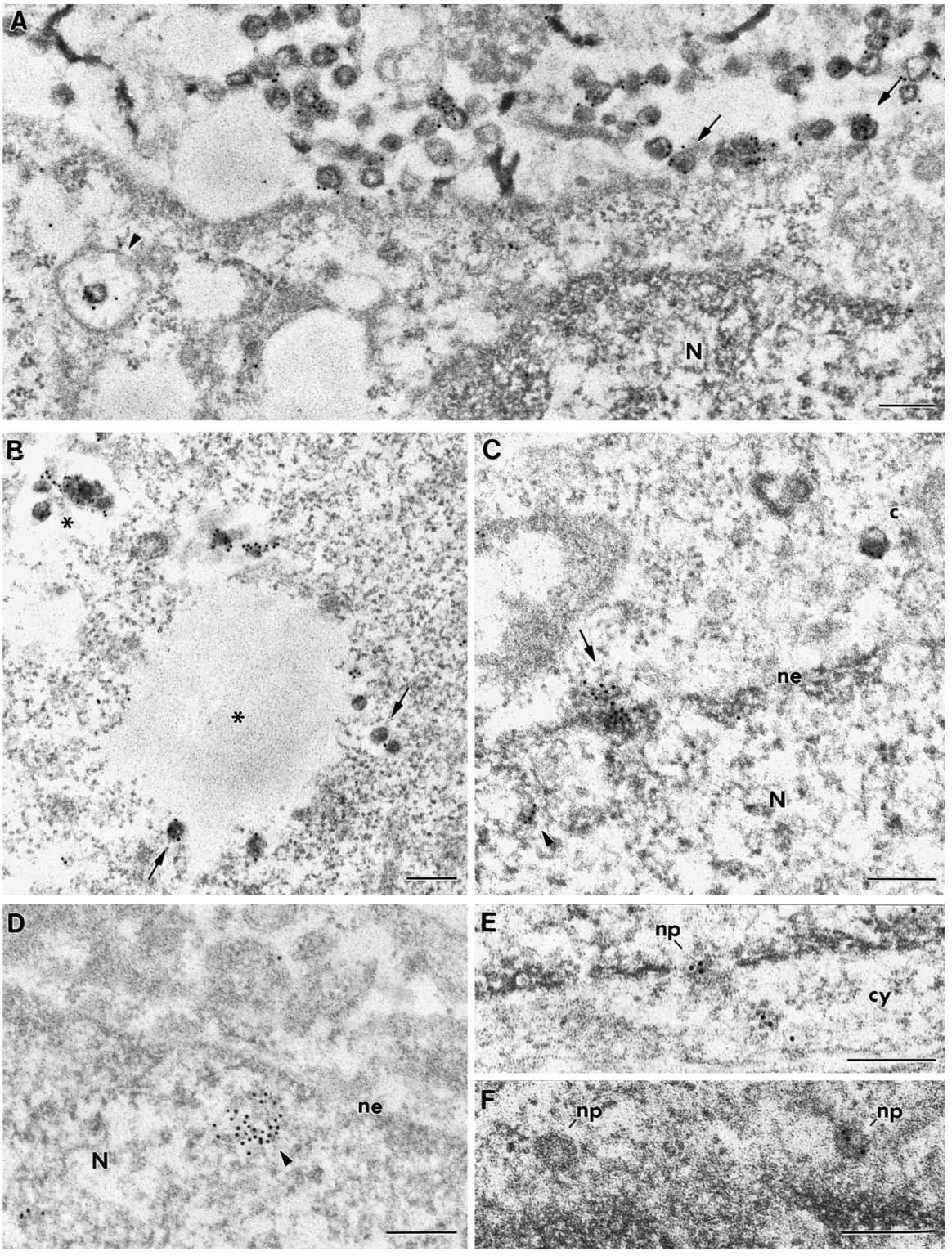

Fig. 3. Immunogold visualization of MuLV uptake and intracellular transport. Lowicryl ultrathin sections of NIH 3T3 cells were processed for immunodetection of NC protein, using a rabbit polyclonal antiserum raised towards the amino-terminal region of this protein. NIH 3T3 samples were obtained 90 minutes after treatment with MuLV. (A) Viruses bound to the plasma membrane (arrows) and inside cytoplasmic vesicles (arrowhead) can be observed. (B) Vesicles (asterisks) containing viruses are disrupted as the virions exit them (arrows) and are released into the cytoplasm. (C) Cytoplasmic cores (c) labeled to localize NC are visualized close to the nuclear envelope (ne) as soon as 30 minutes after incubation with the virus at 37°C, but more often after 90 minutes. Disrupted cores are observed as aggregates of NC-specific label (arrow), close to the nuclear envelope. Simultaneously, NC aggregates (arrowheads in C and D) can be also detected inside the nucleus, not far from the nuclear envelope. (E-F) Immunogold detection of NC shows the presence of this protein associated with nuclear pores (np), either in their center (E, side view) or on their periphery (F, frontal view). N, nucleus; cy, cytoplasm. Bars, 200 nm.

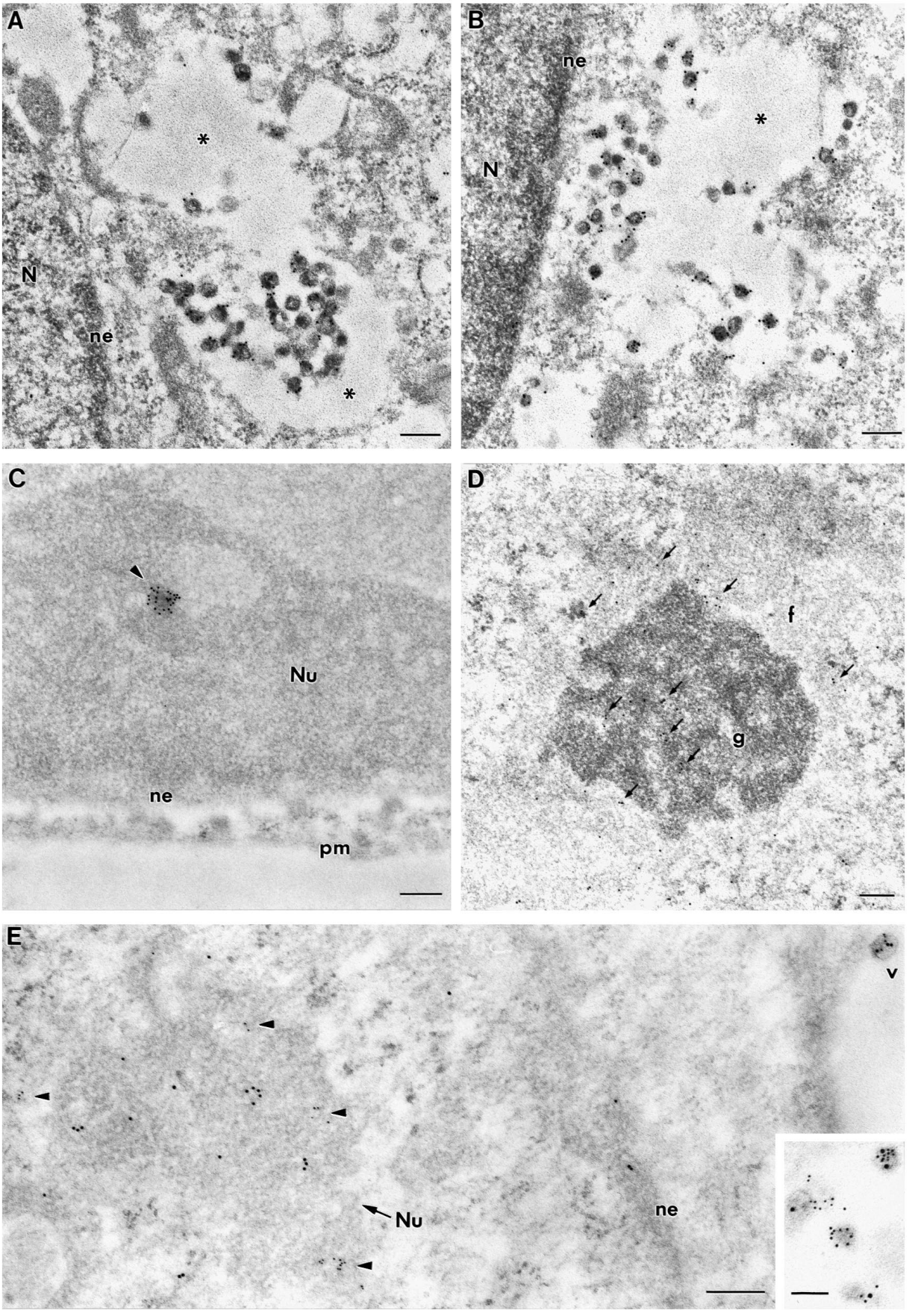
A
N
ne
*
*
B
ne
N
*
C
Nu
ne
pm
D
f
g
E
v
Nu
ne

of the virus to the cell culture, low levels of NC were already detected inside the nucleus of 10% of the cells, but labeling became more significant in samples incubated for 90 minutes at 37°C (Fig. 5). Once inside the nucleus, NC does not spread in a random-like pattern all over the nucleoplasm. Labeling in fibrilar and granular regions of nucleoli is clearly detected in the 60 and 90 minute treatments at 37°C (Fig. 4C,D). After 3 hours, more than 50% of the cells present more NC in nucleoli than in the rest of the nucleus (Fig. 6A). Around 80% of the cells were found to contain NC in their nuclei 10-14 days later, when cells were found to be chronically infected. Intranuclear NC-containing aggregates are depicted by fewer gold particles than extracellular virus or cytoplasmic cores (Fig. 6B). Thus, while more than half of the viruses presented 4-6 10 nm gold particles associated with NC, numerous intranuclear aggregates (62.5%) presented only 3 particles. These data reveal major changes in NC containing structures when entering the nucleus. In fact, these NC aggregates frequently exhibited a linear or ring-like organization inside the nucleus (Fig. 6B, micrographs c-e). It has been proposed that the retroviral protease cleaves the NC protein at its zinc-finger domain in the early stages of the viral replication cycle, and that this cleavage may be crucial for virus infection (Roberts et al., 1991; Nagy et al., 1994). Antibodies against the amino- and carboxyl-terminal regions of NC showed both the same intranuclear distribution of the protein, with preferential location of NC in nucleoli. Simultaneous immunogold labeling using both antisera showed the presence of both antigens inside the nucleus, where they reached the same nucleoli (Fig. 4E). Colocalization of the amino- and carboxyl-terminal regions of NC was observed in around 55% of the viral particles found outside the cell and in the cytoplasm. However, the percentage of intranuclear aggregates showing colocalization of both antigens was remarkably lower (around 10%). This dramatic decrease could be due to conformational changes affecting NC, binding of cellular proteins, or more possibly, to major alterations in the composition of the viral complexes upon entering the nucleus. These results are also consistent with the proposed NC cleavage during the early phase of the virus life cycle.

Fig. 4. Massive arrival of intravesicular MuLV to the nucleus and intranuclear distribution of NC. (A) Vesicles (asterisks) filled with viruses (labeled with a rabbit antiserum specific for the amino-terminal region of NC) are shown approaching the nucleus. (B) When the vesicles are close to the nuclear envelope (ne) the virions move towards the nucleus (N). (C) Discrete aggregates of NC (here labeled with a guinea pig antiserum specific for the carboxyl-terminal region of the protein) are detected (arrowhead) in nucleoli (Nu) of virus-treated cells, mainly 60 or 90 minutes after the incubation with MuLV. (D) Scattered and more intense labeling (here NC was labeled with a rabbit antiserum recognizing its amino-terminal sequence) is usually associated (small arrows) with either fibrilar (f) or granular (g) zones of the nucleolus after 90 minutes and 3 hours. (E) Double labeling of both amino and carboxyl-terminal regions of NC shows that both can be simultaneously visualized in extracellular viruses (v) and intracytoplasmic cores (inset) with different gold particle sizes (5 nm for the amino- and 10 nm for the carboxyl-terminal region). Their co-presence is also detected inside the nucleus, where they reach the same nucleoli. Arrowheads point to 5 nm gold particles. pm, plasma membrane. Bars: 200 nm (80 nm for the inset in E).

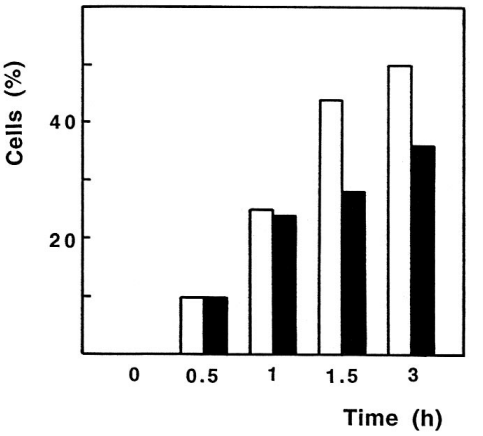

Fig. 5. Immunogold detection of NC and IN in a population of NIH 3T3 cells treated with MuLV for 0, 30, 60, 90 minutes and 3 hours at 37°C. The percentages of cells with significant labeling in the nucleus (defined as those cells having more gold particles in their nucleus than in their cytoplasm) were calculated for NC (open bars) and IN (filled bars), at the times indicated. From 30 to 45 cells were counted for each protein and incubation time.

Release and intranuclear distribution of MuLV IN

The amount of IN present in the virion is low in comparison to the other viral proteins studied (Fig. 1), as a result of the differences in expression between the MuLV polyprotein precursors Gag and Gag-Pol (Luciw and Leung, 1992). IN was labeled using the correponding antiserum and a smaller gold probe (5 nm), to increase the sensitivity of the method (Fig. 7). This yielded an average of 3-5 gold particles per virus in around 50% of the viral particles, as compared with 1-2 gold particles in less than 30% of the viruses when using the 10 nm gold. IN was detected by immunogold labeling in viral cores during their cytoplasmic transport (Fig. 7A). Although the total amount of labeling was lower than with NC due to quantity limitations, intranuclear distribution of IN was similar to that described for NC both in pattern and in its time-course (Fig. 5). IN-containing aggregates, that frequently presented a linear shape as observed for intranuclear NC, were detected in the nucleoplasm (Fig. 7A,B) as well as in nucleoli (Fig. 7C), mainly after incubation for 90 minutes and 3 hours with MuLV at 37°C. Immunogold colabeling of IN and NC (Fig. 7D) was obtained in 17% to 20% of the MuLV virions. At the intranuclear level, both proteins were simultaneously detected in nucleoli (Fig. 7E) although clear colocalization discrete spots were less frequently observed (approximately 10% of the intranuclear aggregates) (Fig. 7F-H). This is probably due to differences in reactivity of the IN and NC antisera, and to differences in the number of IN and NC molecules available for binding by the corresponding antibodies. Our results on the degree of apparent colocalization of NC and IN were similar using antisera recognizing either the amino or the carboxyl-terminal regions of NC.

Immunolocalization of MA and CA

Although several antibodies against MA and CA can successfully label extracellular MuLV particles and intracytoplasmic cores, no detectable amounts of these two proteins were visualized inside the nucleus, at any of the times tested (Fig. 8A,B).

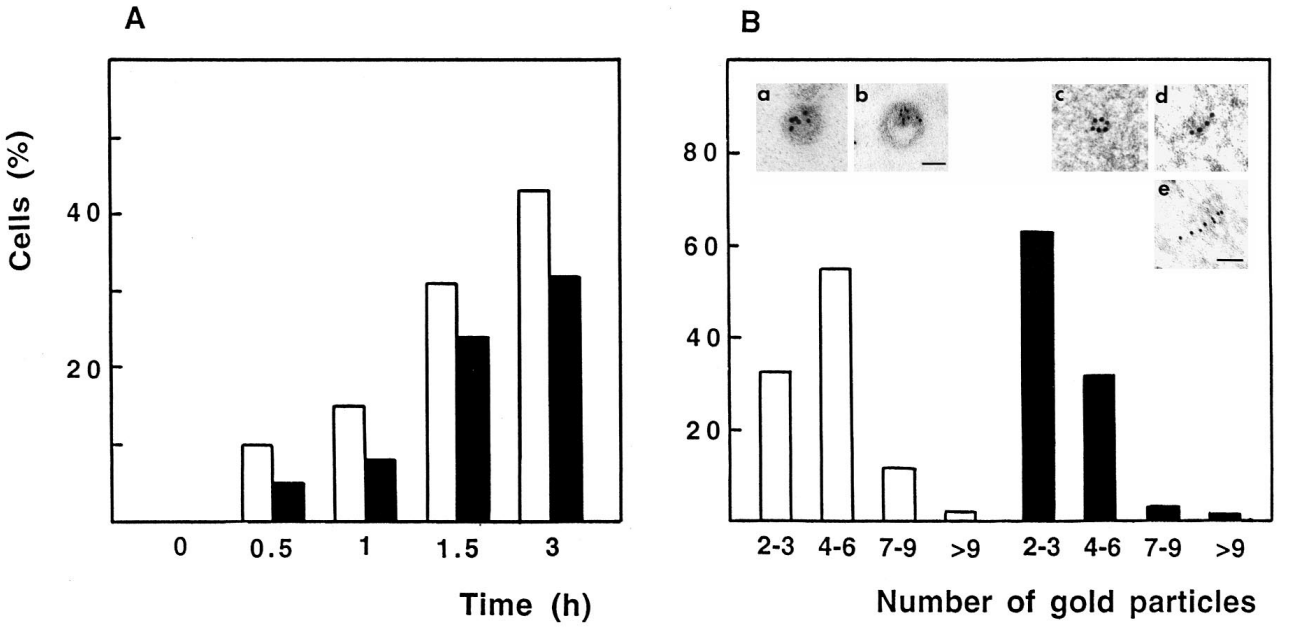

Fig. 6. Progressive intranucleolar accumulation of NC and IN and size variation in NC-containing aggregates after entering the nucleus. (A) The percentage of cells with more labeling of NC (open bars) or IN (filled bars) in nucleoli than in nucleoplasm (defined as those having a larger number of gold particles in their nucleoli than in their nucleoplasm) is shown at different incubation times. (B) The number of 10 nm gold particles associated with NC in intracellular virions (open bars) and in intranuclear aggregates (filled bars) is expressed as percentage of NC-containing structures with a particular number of associated gold particles. Micrographs a,b correspond to immunogold detection of NC in virions, and c-e to intranuclear NC-containing aggregates as visualized by immunolabeling with 10 nm (a, c and d) or 5 nm (b,e) colloidal gold particles. Ring-like (c) or linear (d and e) arrangement of the gold particles in intranuclear aggregates is frequently observed. In (A) from 30 to 45 cells were counted for each protein and time of treatment. In (B) 270 intracellular virions and 219 intranuclear NC aggregates were counted. Bars, 50 nm.

Double immunogold labeling of CA and NC showed that only NC is localized inside nuclei while gold particles associated with CA remained in the cytoplasmic cores (Fig. 8C). Both proteins are clearly co-labeled in extracellular viruses and intracytoplasmic viral particles (Fig. 8C, insets).

DISCUSSION

Immunoelectron microscopy is a powerful technique to follow viral uptake and intracellular changes in viral structures. Our results with MuLV revealed that once inside the cells, the virions that reach the nucleus were apparently devoid of their envelope but remained as intact cores. These viral capsids appear to be rather stable in the cytoplasmic environment, in contrast to HIV cores, which are disrupted shortly after fusion with the plasma membrane (Grewe et al., 1990). MuLV intracytoplasmic cores contained similar amounts of MA, CA, NC and IN to those in the capsids of extracellular virions, as estimated by immunogold labeling. Interestingly, the MuLV preintegration complexes isolated from the cytoplasm of acutely infected cells were shown to contain the viral proteins CA and IN, and had a relatively large size in comparison to ribosomes (Bowerman et al., 1989). However, their apparent sedimentation coefficient (160 S) was smaller than that reported for MuLV mature cores (350 S), by Yoshinaka and Luftig (1977). Our immunoelectron microscopy study suggests that they could be altered or partially disassembled viral capsids. MuLV cores were frequently observed in the cytoplasm, in the proximity of the nuclear membrane, and close to nuclear pores, but never in the nucleoplasm. Nuclear import of NC and IN was detected soon after exposure of the cells to the virus, while MA and CA were always found only in the cytoplasm.

Mitosis is known to be essential for integration in oncoretroviruses (Hajihosseini et al., 1993; Lewis and Emerman, 1994; Roe et al., 1993), but not for HIV which can infect non-dividing cells (Lewis et al., 1992). The differences between MuLV and HIV have been explained by either proposing the existence of 'licensing' factors (proteins whose nuclear vs cytoplasmic distribution is cell cycle-regulated), or assuming that the large size of the MuLV preintegration complexes

Fig. 7. Immunogold labeling of IN. (A-B) A rabbit polyclonal antiserum and a secondary antibody conjugated with 5 nm colloidal gold revealed the location of IN in intracellular virions (v) and inside the nucleus (N). Intranuclear IN aggregates (arrows in A and B) frequently have a linear shape. (C) Labeling corresponding to IN was also localized in nucleoli (Nu) of cells treated with the virus (here, 90 minutes after treatment). Small (arrow) and bigger (arrowhead) groups of gold particles can be seen. (D) Double labeling of IN (5 nm) and NC (10 nm) is observed in the viral particles (arrow). (E) Inside the cells treated with the virus, NC and IN can be detected in the fibrilar (f) and granular (g) regions of the nucleoli, although intranuclear colocalization spots (F-H) are occasionally detected. In micrographs D-H, NC was labeled with a guinea pig antiserum recognizing the carboxyl-terminal region of NC and a 10 nm gold conjugate, while IN was visualized with 5 nm gold particles (arrowheads). ne, nuclear envelope. Bars, 100 nm.

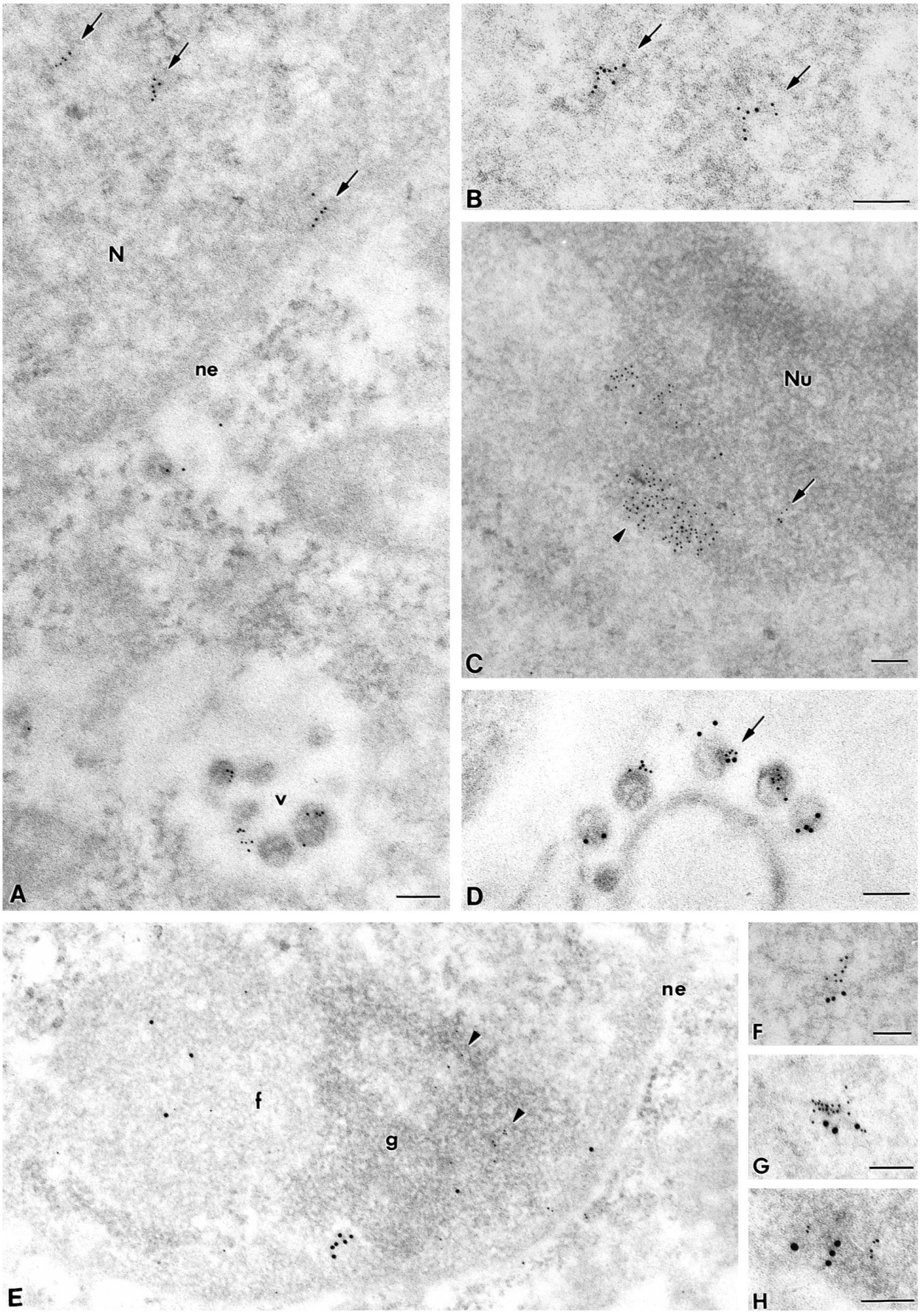
N
ne
v
A
B
Nu
C
D
ne
f
g
E
F
G
H

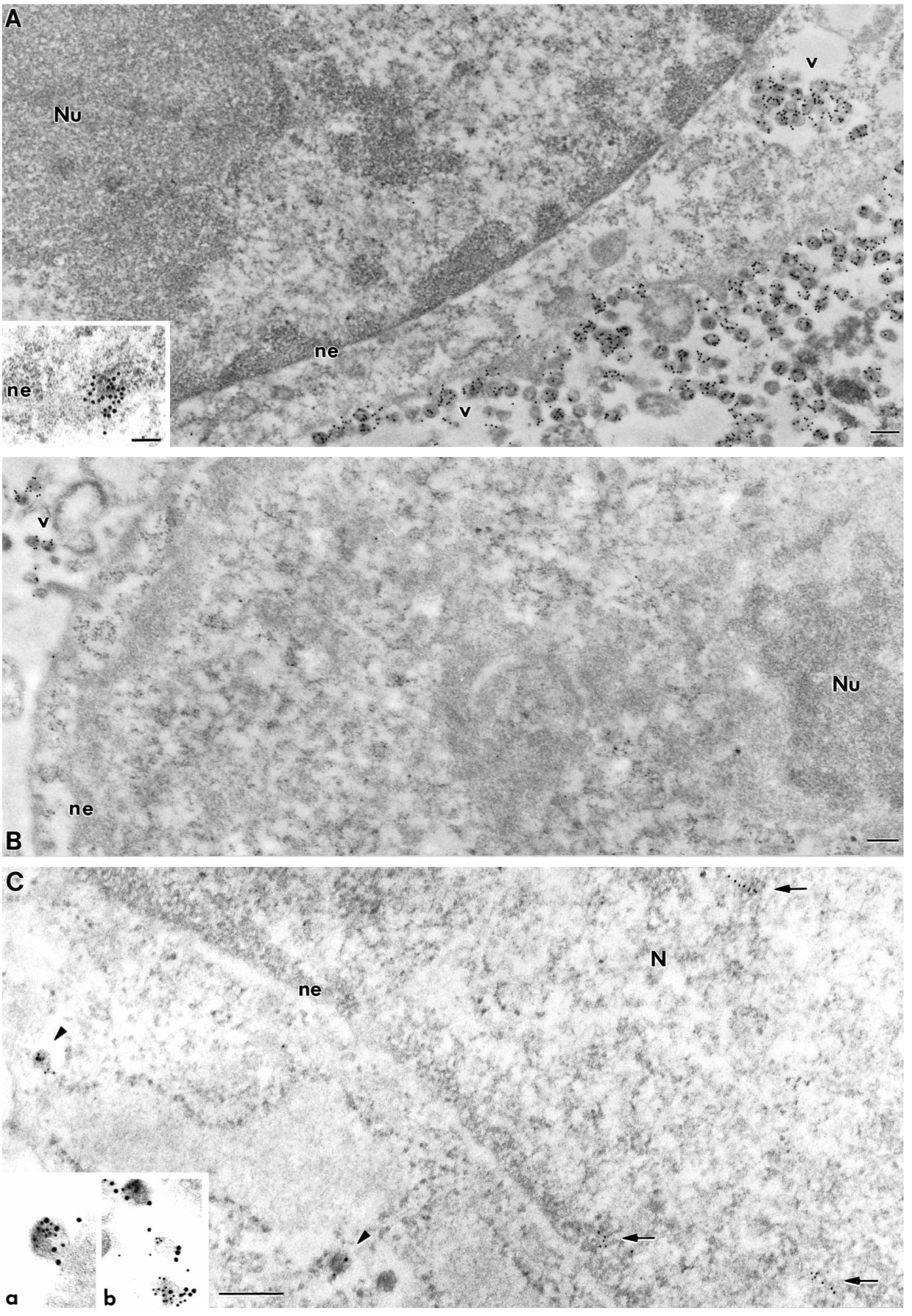
A
Nu
v
ne
v
ne
B
v
Nu
ne
C
N
ne
a
b

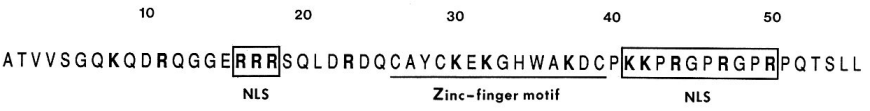

Fig. 9. Amino acid sequence of Moloney-MuLV NC, showing the location of lysines and arginines (bold), the potential nuclear localization signals (NLS), and the zinc-finger motif.

would prevent them from entering the nucleus, an event which could take place after breakdown of the nuclear membrane during mitosis (Roe et al., 1993). Nevertheless, electron microscopy studies have demonstrated that large viral particles (i.e. SV40; mean diameter, 50 nm) can enter the nucleus through the nuclear pores (Yamada and Kasamatsu, 1993), or after fusion of the endosomal membrane with the nuclear envelope (Mackay and Consigli, 1976; Nishimura et al., 1986). Transport through the nuclear pore occurs by an ATP-dependent process which requires a specific nuclear localization signal (Gerace, 1992). These signals are usually formed by short basic sequence motifs (García-Bustos et al., 1991), and have been found in several proteins of DNA viruses (Kalderon et al., 1984; Lyons et al., 1987), as well as in retroviral *trans*-activating proteins, such as HIV-1 Tat and Rev, and HTLV-I Rex (Cullen et al., 1988; Kubota et al., 1991; Siomi et al., 1988). Bukrinsky et al. (1992) have shown that HIV-1 preintegration complexes enter the nucleus by an ATP-dependent process, which appears to be mediated by a nuclear localization signal found in MA (Bukrinsky et al., 1993). Nuclear targeting signals have not been experimentally identified in MuLV proteins, although we could detect NC and IN associated with the nuclear pores. Both proteins are basic, but a functional IN does not appear to be a requirement for nuclear localization of retroviral DNA since IN deficient mutants of MuLV direct the formation of all nuclear forms of viral DNA (Schwartzberg et al., 1984). On the other hand, NC contains potential nuclear localization signals, at positions 16-18 and 41-50, adjacent to the zinc-finger motif (Fig. 9). Interestingly, replacement of these basic residues by neutral ones did not impair Moloney-MuLV assembly, production and maturation in vivo, but the obtained viruses were poorly infectious (Housset et al., 1993), suggesting their involvement in events occurring during the early phase of the virus life cycle. Our results do not prove that NC and IN are transported into the nucleus as part of the same complexes, since immunogold colabeling of NC and IN was occasionally observed even in single mature viral particles. However, both proteins share the same entry pathway and appear to be directed to the same intranuclear compartments. This suggests that they could be cotransported inside the nucleus. In addition, NC and IN contain zinc-finger motifs, which are likely to be involved in viral nucleic acid binding (Bushman et al., 1993; Gorelick et al., 1988; Khan et al., 1991; Méric and Goff, 1989). The linear arrangement of the immunogold label associated with NC and IN inside the nucleus, could reflect the interaction of these proteins with extended forms of viral DNA inside the nucleus. Nevertheless, until we develop a method to simultaneously detect specific viral DNA and associated proteins at the EM level, the question of whether these structures are indeed preintegration complexes remains unsolved.

Our immunoelectron microscopy study also reveals that NC and IN are both targeted to the nucleoli of NIH 3T3 cells. Other retroviral proteins, such as HIV Rev and HTLV Rex are also targeted to the nucleolus with the participation of specific nucleolar localization signals (Cullen et al., 1988; Kubota et al., 1991; Siomi et al., 1988). These signals are recognized by a mammalian nuclear shuttle protein known as B23, which binds specifically to HIV-1 Rev (Fankhauser et al., 1991) and HTLV-I Rex (Adachi et al., 1993). B23, as well as other nucleolar shuttle proteins, play an important role in ribosome biogenesis, through its involvement in the nucleocytoplasmic transport of ribosomal components (Borer et al., 1989; Nigg et al., 1991).

The biological relevance of all observations is compromised by the difficulties of distinguishing between an infectious and a noninfectious particle. It is possible that most of the deenveloped viruses found in the cytoplasm of newly infected cells will not actively participate in infection. However, those NC- and IN-containing particles that enter the nucleus are likely to be involved in this process. Nevertheless, further studies will be necessary to assess the significance of the new findings obtained in this report, such as the nuclear import of the nucleocapsid protein during retroviral infection and the targeting of NC and IN to the nucleolus.

We express our gratitude to Pat Wesdock and Suzanne Specht for help with peptide synthesis and antibody production, and to Alan Rein, José L. Carrascosa, and Esteban Domingo for valuable suggestions. The content of this publication does not necessarily reflect the views or policies of the Department of Health and Human Services, nor does mention of trade names, commercial products, or organization imply endorsement by the U.S. Government. Research sponsored in part by the National Cancer Institute, DHHS under contract No. NO1-CO-74101 with ABL.

Fig. 8. Immunogold labeling of CA (A) and MA (B) in cells treated 90 minutes with MuLV. Labeling can be seen in extracellular and intracellular virions (v), as well as associated with viral remains at the nuclear envelope (inset in A), but a detectable amount of these two proteins was never seen inside the nucleus. (C) Simultaneous localization of NC and CA shows that in cells treated 90 minutes with MuLV only the NC protein (here labeled with a rabbit antiserum against the amino-terminal of the protein and 5 nm gold particles) enters the nucleus (arrows), while CA (detected with a guinea-pig antiserum and 10 nm gold particles) remains associated with cytoplasmic viral structures (arrowheads and inset 'b'). Inset 'a' shows double labeling of CA and NC in an extracellular virion. N, nucleus; Nu, nucleolus; ne, nuclear envelope. Bars: 200 nm; inset in A, 75 nm; inset 'a' in C, 120 nm; inset 'b' in C, 150 nm.

REFERENCES

Adachi, Y., Copeland, T., Hatanaka, M. and Oroszlan, S. (1993). Nucleolar targeting signal of rex protein of human T-cell leukemia virus type I specifically binds to nucleolar shuttle protein B-23. *J. Biol. Chem.* **268**, 13930-13934.

Andersen, K. B. and Nexø, B. A. (1983). Entry of murine retroviruses into mouse fibroblasts. *Virology* **125**, 85-98.

Borer, R. A., Lehner, C. F., Eppenberger, H. M. and Nigg, E. A. (1989). Major nucleolar proteins shuttle between nucleus and cytoplasm. *Cell* **56**, 379-390.

Bowerman, B., Brown, P. O., Bishop, J. M. and Varmus, H. E. (1989). A

nucleoprotein complex mediates the integration of retroviral DNA. *Genes Dev.* **3**, 469-478.

Bukrinsky, M. I., Sharova, N., Dempsey, M. P., Stanwick, T. L., Bukrinskaya, A. G., Haggerty, S. and Stevenson, M. (1992). Active nuclear import of human immunodeficiency virus type 1 preintegration complexes. *Proc. Nat. Acad. Sci. USA* **89**, 6580-6584.

Bukrinsky, M. I., Haggerty, S., Dempsey, M. P., Sharova, N., Adzhubei, A., Spitz, L., Lewis, P., Goldfarb, D., Emerman, M. and Stevenson, M. (1993). A nuclear localization signal within HIV-1 matrix protein that governs infection of non-dividing cells. *Nature* **365**, 666-669.

Bushman, F. D., Engelman, A., Palmer, I., Wingfield, P. and Craigie, R. (1993). Domains of the integrase protein of human immunodeficiency virus type 1 responsible for polynucleotidyl transfer and zinc binding. *Proc. Nat. Acad. Sci. USA* **90**, 3428-3432.

Carrascosa, J. L., González, P., Carrascosa, A. L., García-Barreno, B., Enjuanes, L. and Viñuela, E. (1986). Localization of structural proteins in African Swine Fever virus particles by immunoelectron microscopy. *J. Virol.* **58**, 377-384.

Carrascosa, J. L. (1988). Immunoelectron microscopical studies on viruses. *Electron Microsc. Rev.* **1**, 1-16.

Cullen, B. R., Hauber, J., Campbell, K., Sodroski, J. G., Haseltine, W. A. and Rosen, C. A. (1988). Subcellular localization of the human immunodeficiency virus *trans*-acting *art* gene product. *J. Virol.* **62**, 2498-2501.

Fankhauser, C., Izaurralde, E., Adachi, Y., Wingfield, P. and Laemmli, U. K. (1991). Specific complex of human immunodeficiency virus type 1 Rev and nucleolar B23 proteins: Dissociation by the rev responsive element. *Mol. Cell. Biol.* **11**, 2567-2575.

Fu, W. and Rein, A. R. (1993). Maturation of dimeric viral RNA of Moloney murine leukemia virus. *J. Virol.* **67**, 5443-5449.

García-Bustos, J., Heitman, J. and Hall, M. N. (1991). Nuclear protein localization. *Biochim. Biophys. Acta* **1071**, 83-101.

Gelderblom, H. R., Hausmann, E. H. S., Ozel, M., Pauli, G. and Koch, M. A. (1987). Fine structure of human immunodeficiency virus (HIV) and immunolocalization of structural proteins. *Virology* **156**, 171-176.

Gerace, L. (1992). Molecular trafficking across the nuclear pore complex. *Curr. Opin. Cell Biol.* **4**, 637-645.

Gorelick, R. J., Henderson, L. E., Hanser, J. P. and Rein, A. (1988). Point mutants of Moloney murine leukemia virus that fail to package viral RNA: Evidence for specific RNA recognition by a 'zinc finger-like' protein sequence. *Proc. Nat. Acad. Sci. USA* **85**, 8420-8424.

Grewe, C., Beck, A. and Gelderblom, H. R. (1990). HIV: Early virus-cell interactions. *J. Acquired Immune Defic. Syndr.* **3**, 965-974.

Hajihosseini, M., Iavachev, L. and Price, J. (1993). Evidence that retroviruses integrate into post-replication host DNA. *EMBO J.* **12**, 4969-4974.

Housset, V., De Rocquigny, H., Roques, B. P. and Darlix, J.-L. (1993). Basic amino acids flanking the zinc finger of Moloney murine leukemia virus nucleocapsid protein NCp10 are critical for virus infectivity. *J. Virol.* **67**, 2537-2545.

Kalderon, D., Roberts, B. L., Richardson, W. D. and Smith, A. E. (1984). A short amino acid sequence able to specify nuclear location. *Cell* **39**, 499-509.

Kellenberger, E. and Hayat, M. A. (1991). Some basic concepts for the choice of methods. In *Colloidal gold. Principles, Methods, and Applications* (ed. M. A. Hayat), pp. 1-30. Academic Press, Ltd, London.

Khan, E., Mack, J. P. G., Katz, R. A., Kulkosky, J. and Skalka, A. M. (1991). Retroviral integrase domains: DNA binding and the recognition of LTR sequences. *Nucl. Acid Res.* **19**, 851-860.

Kubota, S., Nosaka, T., Cullen, B. R., Maki, M. and Hatanaka, M. (1991). Effects of chimeric mutants of human immunodeficiency virus type 1 Rev and human T-cell leukemia virus type I Rex on nucleolar targeting signals. *J. Virol.* **65**, 2452-2456.

Lewis, P., Hensel, M. and Emerman, M. (1992). Human immunodeficiency virus infection of cells arrested in the cell cycle. *EMBO J.* **11**, 3053-3058.

Lewis, P. F. and Emerman, M. (1994). Passage through mitosis is required for oncoretroviruses but not for the human immunodeficiency virus. *J. Virol.* **68**, 510-516.

Luciw, P. A. and Leung, N. J. (1992). Mechanisms of retrovirus replication. In *The Retroviridae*, vol. I (ed. J. A. Levy), pp. 159-298. Plenum Press, New York.

Lyons, R. H., Ferguson, B. Q. and Rosenberg, M. (1987). Pentapeptide nuclear localization signal in adenovirus E1a. *Mol. Cell. Biol.* **7**, 2451-2456.

Mackay, R. L. and Consigli, R. A. (1976). Early events in polyoma virus infection: Attachment, penetration, and nuclear entry. *J. Virol.* **19**, 620-636.

Marsh, M. and Helenius, A. (1989). Virus entry into animal cells. *Advan. Virus Res.* **36**, 107-151.

Menéndez-Arias, L., Risco, C., Pinto Da Silva, P. and Oroszlan, S. (1992). Purification of immature cores of mouse mammary tumor virus and immunolocalization of protein domains. *J. Virol.* **66**, 5615-5620.

Méric, C. and Goff, S. P. (1989). Characterization of Moloney murine leukemia virus mutants with single-amino-acid substitutions in the Cys-His box of the nucleocapsid protein. *J. Virol.* **63**, 1558-1568.

Miyamoto, K. and Gilden, R. (1971). Electron microscopy studies of tumor viruses. 1. Entry of murine leukemia virus into mouse embryo fibroblasts. *J. Virol.* **7**, 395-406.

Nagy, K., Young, M., Baboonian, C., Merson, J., Whittle, P. and Oroszlan, S. (1994). Antiviral activity of human immunodeficiency virus type 1 protease inhibitors in a single cycle of infection: evidence for a role of protease in the early phase. *J. Virol.* **68**, 757-765.

Nigg, E. A., Baeuerle, P. A. and Lührmann, R. (1991). Nuclear import-export: In search of signals and mechanisms. *Cell* **66**, 15-22.

Nishimura, T., Kawai, N., Kawai, M., Notake, K. and Ichihara, I. (1986). Fusion of SV40-induced endocytic vacuoles with the nuclear membrane. *Cell Struct. Funct.* **11**, 135-141.

Poiesz, B. J., Ruscetti, F. W., Gazdar, A. F., Bunn, P. A., Minna, J. D. and Gallo, R. C. (1980). Detection and isolation of type C retrovirus particles from fresh and cultured lymphocytes of a patient with cutaneous T-cell lymphoma. *Proc. Nat. Acad. Sci. USA* **77**, 7415-7419.

Ragheb, J. A. and Anderson, W. F. (1994). pH-independent murine leukemia virus ecotropic envelope-mediated cell fusion: implications for the role of the R peptide and p12E TM in viral entry. *J. Virol.* **68**, 3220-3231.

Risco, C., Carrascosa, J. L. and Bosch, M. A. (1991). Uptake and cellular distribution of Escherichia coli lipopolysaccharide by isolated rat type II pneumocytes. *J. Histochem. Cytochem.* **39**, 607-615.

Risco, C. and Pinto da Silva, P. (1993). Binding of bacterial endotoxins to the macrophage surface: Visualization by fracture-flip and immunocytochemistry. *J. Histochem. Cytochem.* **41**, 601-608.

Risco, C., Romero, C., Bosch, M. A. and Pinto da Silva, P. (1994). Rat type II pneumocytes revisited: Intracellular membranous systems, surface characteristics, and lamelar body secretion. *Lab. Invest.* **70**, 407-417.

Risco, C. and Pinto da Silva, P. (1995). Cellular functions during activation and damage by pathogens: Immunogold studies of the interaction of bacterial endotoxins with target cells. *Microsc. Res. Tech.* **31**, 141-158.

Roberts, M. M., Copeland, T. D. and Oroszlan, S. (1991). In situ processing of a retroviral nucleocapsid protein by the viral proteinase. *Prot. Engineer* 4, 695-700.

Roe, T., Reynolds, T. C., Yu, G. and Brown, P. O. (1993). Integration of murine leukemia virus DNA depends on mitosis. *EMBO J.* **12**, 2099-2108.

Schwartzberg, P., Colicelli, J. and Goff, S. P. (1984). Construction and analysis of deletion mutations in the *pol* gene of Moloney murine leukemia virus: A new viral function required for productive infection. *Cell* **37**, 1043-1052.

Siomi, H., Shida, H., Nam, S. H., Nosaka, T., Maki, M. and Hatanaka, M. (1988). Sequence requirements for nucleolar localization of human T cell leukemia virus type I pX protein, which regulates viral RNA processing. *Cell* **55**, 197-209.

Varmus, H. and Swanstrom, R. (1982). Replication of retroviruses. In *RNA Tumor Viruses* (ed. R. Weiss, N. Teich, H. Varmus and J. Coffin), pp. 369-512. Cold Spring Harbor Laboratory, Cold Spring Harbor, New York.

Yamada, M. and Kasamatsu, H. (1993). Role of nuclear pore complex in simian virus 40 nuclear targeting. *J. Virol.* **67**, 119-130.

Yoshinaka, Y. and Luftig, R. B. (1977). Murine leukemia virus morphogenesis: Cleavage of p70 *in vitro* can be accompanied by a shift from a concentrically coiled internal strand ('immature') to a collapsed ('mature') form of the virus core. *Proc. Nat. Acad.Sci. USA* **74**, 3446-3450.

(Received 28 April 1995 - Accepted 2 June 1995)